Journal of Analytical and Applied Pyrolysis 117 (2016) 157–161

Contents lists available at ScienceDirect

Journal of Analytical and Applied Pyrolysis

journal homepage: www.elsevier.com/locate/jaap

Synthesis, characterization and thermal behaviour of solid alkali metal mandelates in pyrolytic and oxidant atmosphere

R.C. Silva [a,*], F.J. Caires [b], D.J.C Gomes [c], T.A.D. Colman [d], M. Ionashiro [d]

[a] Faculdade de Ciências Agronômicas, Universidade Estadual Paulista, 18.603-970 Botucatu, São Paulo, Brazil
[b] Departamento de Química, Universidade Estadual Paulista, 17033-260, Bauru, São Paulo, Brazil
[c] Instituto Federal de Educação, Ciência e Tecnologia do Piauí, Campus Paulistania: Rod. Br-407, s/n Centro, Paulistânia, Piauí, Brazil
[d] Instituto de Química, Universidade Estadual Paulista, 14801-970 Araraquara, SP, Brazil

ARTICLE INFO

Article history:
Received 11 September 2015
Received in revised form 28 October 2015
Accepted 21 November 2015
Available online 9 December 2015

Keywords:
Alkali metals
Mandelate
Thermal behaviour
TG-DSC coupled to FTIR

ABSTRACT

Characterization, thermal stability and thermal decomposition of alkali metal mandelates, $M(C_6H_5CH(OH)CO_2)nH_2O$ (where M represents Na, K, Rb and Cs and $n = 0.3$ (Na), 0.6 (K), 2 (Rb) and 1 (Cs)) were investigated employing simultaneous thermogravimetry and differential scanning calorimetry (TG-DSC), atomic absorption spectrophotometry (AA), X-ray diffractometry and TG-DSC coupled to infrared spectrophotometer (FTIR). For all the compounds, the mass loss occurs in the beginning of the TG-DSC curves. In the nitrogen atmosphere it was observed that the mass loss of the anhydrous compounds occurs in four or five steps and the mass loss is still observed up to 1000 °C, except for the anhydrous compounds under dynamic dry air atmosphere, after the first three steps occurs with the formation of the respective carbonate. The results also provided information concerning the thermal stability and decomposition as well as identification of the gaseous products evolved during the thermal decomposition of these compounds.

1. Introduction

Mandelic acid is an aromatic alpha hydroxyl acid with the molecular formula $C_6H_5CH(OH)CO_2H$ and it has a long history as antibacterial, particularly in treatment of urinary tract infectious [1]. It has been reported in the literature some work about mandelic acid and their compounds, as shown: studies of some bivalent solid complexes of iron [2], infrared spectrum of mandelate complex of nickel II [3], the complexation of mandelates of lanthanide [4], magnesium bis[D(−)mandelate] anhydrous and other alkaline earth, alkali and zinc salts of mandelic acid [5], mixed-ligand complexes of copper (II) with α-hydroxycarboxylic acid and 1,10-phenanthroline [6], synthesis, structures and magnetic properties of layered bivalent metal mandelates [7] mononuclear, dinuclear and hidroxo-briged tetranuclear complexes from reactions of Cu (II) ions, mandelic acid diimina ligands [8] and synthesis, characterization and thermal study of solid-state alkaline earth mandelates, except beryllium and radium [9]. In this paper, the object of the present research was to prepare solid-state compounds of alkali metal mandelates (i.e. Na, K, Rb and Cs) and to investigate by means of atomic absorption (AA), infrared spectroscopy (FTIR), simultaneous thermogravimetry and differential thermal analysis (TG-DTA) under air atmosphere, differential scanning calorimetry (DSC) and TG-DSC, under nitrogen atmosphere, coupled to FTIR.

2. Experimental

The mandelic acid, $C_6H_5CH(OH)CO_2H$ with 99% purity was obtained from Sigma and it was used as received.

Solid-state alkali metal mandelates were obtained by neutralization of sodium hydroxide 0.2 mol L^{-1} or potassium, rubidium and caesium carbonates 0.1 mol L^{-1} (100 mL) with mandelic acid solutions. Solutions were evaporated to near dryness in a water bath, dried at 50 °C in a forced circulation air oven (12 h) and kept in a desiccator over anhydrous calcium chloride.

In the solid-state, metal ions were determined by using atomic absorption spectrophotometer HR-CSF AAS, from Analytik Jena Contr AA 300.

Water content was determined from TG curves, and ligand lost was also determined from TG curves, based on the mass losses up to the temperature where the respective carbonates are formed.

X-ray powder patterns were obtained by using a Siemens D5000 X-ray diffractometer employing CuKα Radiation (λ = 1.541 Å) and setting of 40 kV and 20 mA.

* Corresponding author.
E-mail address: ritaquimica@gmail.com (R.C. Silva).

http://dx.doi.org/10.1016/j.jaap.2015.11.017
0165-2370/

Simultaneous TG-DSC curves were obtained by using TG-DSC STARe system, from Mettler Toledo.

The purge gas was an air and/or Nitrogen flow of 50 mL min^{-1} and heating rate of 10 °C min^{-1} was adopted with samples weighing about 12 mg. Platinum crucibles were used for recording the TG-DSC curves.

The monitoring of gaseous products were carried out using TG-DSC 1 Mettler Toledo coupled to FTIR spectrophotometer Nicolet with gas cell and DTG S KBr detector. The furnace and heated gas cell (250 °C) were coupled through a heated (200 °C) 120 cm stainless steel line transfer with diameter of 3 mm, both purged with dry air (50 mL min^{-1}). The FTIR spectra were recorded with 16 scans per spectrum at a resolution of 4 cm^{-1}.

The morphology of sample holder was observed using a high resolution field-emission gun scanning electron microscopy FEG-SEM (Supra 35-VP, Carl Zeiss, Germany).

3. Results and discussion

The analytical and thermoanalytical (TG), under air atmosphere, results are shown in Table 1. From these data the stoichiometry of these compounds could be established, as shown in succession. For sodium compound, as example:

$$H_20 = 2.84\% \div 18.02^* = 0.158 \div 0.5592 = 0.3$$

$$^*H_2O = 18.02$$

$$\Delta L = 67.86\% \div 121.145^{**} = 0.5602 \div 0.5592 = 1.00$$

$$^{**} NaL - 0.5\ Na_2CO_3 = 121.145$$

$$0.5\ Na_2O = 17.33\% \div 30.99^{***} = 0.5592 \rightarrow (1)$$

$$^{***} 0.5\ Na_2O = 30.99$$

$$Na(L).0.3\ H_2O$$

Thus, the general formula of these compounds: $M(L)\cdot nH_2O$ where M represents Na, K, Rb and Cs; L is mandelate and $n = 0.3$ (Na), 0.6 (K), 2 (Rb) and 1 (Cs). All the compounds are hygroscopic, and the hygroscopicity of these compounds follows the order: Rb > Cs > K > Na.

The X-ray diffraction powder patterns in Fig. 1 shows that the sodium and potassium compounds have a crystalline structure, without evidence of formation of isomorphous ones. For rubidium and caesium the X-ray diffraction powder patterns was not obtained due to the high hygroscopicity of these compounds.

The TG-DSC curves of the compounds in dynamic dry air atmosphere are shown in Fig. 2. These curves show mass losses in five or six steps and thermal events corresponding to these losses or due to physical phenomenon. These curves also show that the mass loss due to dehydration occurs for all the compounds in the beginning of the TG-DSC curves (40 °C), in spite of the compounds have been maintained at 50 °C in a forced circulation air oven during 12 h and kept in a desiccator over anhydrous calcium chloride up to dryness. Thus the dehydration occurred in the beginning of the TG-DSC curves because these compounds are hygroscopic. For potassium and rubidium compounds the dehydration occurs in two consecutive steps and for sodium and caesium ones the dehydration occurs in a single step and through a slow process.

The thermal stability of the anhydrous compounds shown by TG-DSC curves depends on the nature of the metal ion and they follow the order:

K > Na > Rb > Cs

Only for caesium compounds the TG-DSC curves show that the final thermal decomposition occurs under to 950 °C, while for sodium, potassium and rubidium compounds these curves show that the mass losses are still being observed up to 1000 °C.

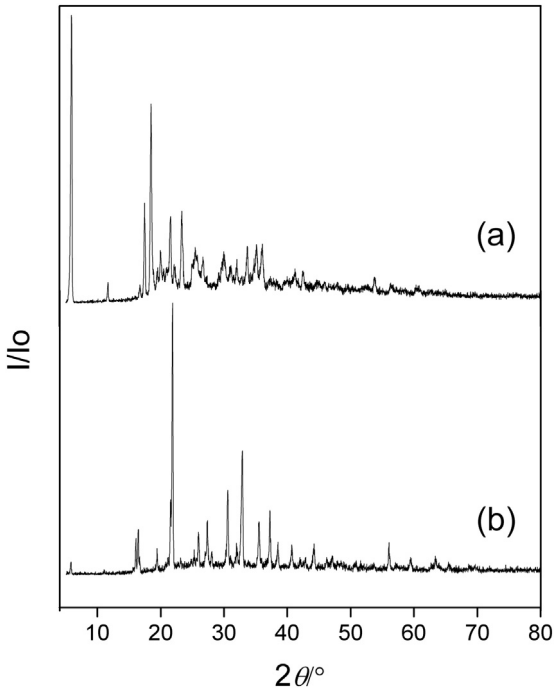

Fig. 1. X-ray powder diffraction patterns of the compounds: (a) NaL and (b) KL (L = mandelate).

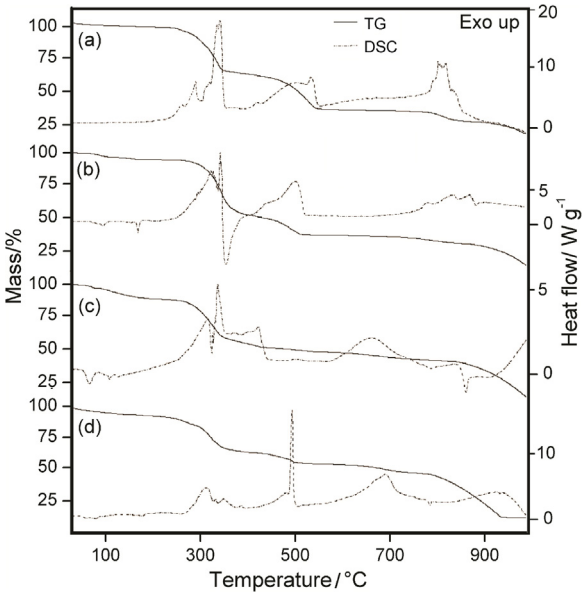

Fig. 2. Simultaneous TG-DSC curves of the compounds in dry air atmosphere: (a) NaL (m = 12.1800 mg), (b) KL (m = 12.0730 mg), (c) RbL (m = 12.1000 mg), (d) CsL (m = 12.0060 mg) under dry air atmosphere.

The percent of ligand and metals were determined by stoichiometry calculations, based on thermal analysis and atomic absorption, respectively.

The thermal behaviour of the compounds is also dependent on the nature of the metal ion and so the features of each of these compounds are discussed individually.

3.1. Sodium compound

The TG-DSC curves are shown in Fig. 2(a). The first mass loss between 40 and 190 °C is attributed to dehydration with loss of

Table 1
Analytical and thermoanalytical (TG) results for M(L)·nH_2O compounds.

Compounds	M oxide/(%)		L lost/(%)		C/(%)		H/(%)		H_2O/(%)		Residue (T/°C)
	Calcd.	A.A.	Calcd.	TG[a]	Calcd.	EA.	Calcd.	EA	Calcd.	TG[a]	
Na(L)·0.3H_2O	17.26	17.33	67.47	67.86	53.51	53.03	4.28	4.03	3.01	2.84	Na_2CO_3 (850)
K(L)·0.6H_2O	23.43	23.28	60.24	60.88	47.79	48.29	4.12	4.30	5.38	5.12	K_2CO_3 (850)
Rb(L)·2H_2O	34.28	34.59	43.57	44.00	35.24	35.55	4.07	4.31	13.22	13.00	Rb_2CO_3 (720)
Cs(L)·1H_2O	46.64	47.04	40.10	40.74	31.81	31.11	3.01	2.98	5.97	6.00	Cs_2CO_3 (730)

M = alkali metal; L = mandelate.
[a] TG in dynamic dry air atmosphere.

0.3 H_2O (Calcd. = 3.01%; TG = 2.84%). No thermal event corresponding to dehydration is observed in the DSC curve, undoubtedly because the small mass loss occurs slowly which the heat absorbed is not sufficient to produce a thermal event.

The anhydrous compound is stable up to 240 °C and above this temperature, the first two mass losses between 240 and 350 °C and 350–550 °C, with losses of 31.29% and 27.15%, corresponding to exothermic peaks at 260, 290, 330, 335 °C and 420, 500, 530 °C, respectively, are attributed to oxidation of the organic matter and/or of the gaseous products evolved during the thermal decomposition, with formation of sodium carbonate and/or carbonaceous residue.

The third mass loss between 640 and 850 °C, with loss of 9.42%, corresponding to exothermic peaks at 805 and 820 °C are attributed to the oxidation of carbonaceous residue, from sodium carbonate (Calcd. = 70.48%; TG = 70.70%). The last mass loss above 850 °C up to 1000 °C is attributed to evaporation and/or thermal decomposition of sodium carbonate. In the last endothermic peak the shoulder at 840 °C, it seems to be to the melting of sodium carbonate.

For the all obtained compounds the carbonaceous residue was identified by using qualitative test with diluted HCl solution with evolution CO_2.

3.2. Potassium compound

The TG-DSC curves are shown in Fig. 2(b). The first two mass losses between 40 and 120 °C and 120–170 °C, corresponding to endothermic peaks at 100 and 160 °C, respectively are attributed to dehydration with losses of 0.4 and 0.2 H_2O (Calcd. = 3.58 and 1.80%; TG = 3.42 and 1.70%). The endothermic peak at 172 °C is attributed to the fusion of the compound.

The anhydrous compound is stable up to 260 °C and above this temperature the first two mass losses between 260 and 390 °C and 390–520 °C, with losses of 43.21% and 14.82%, corresponding to exo and endothermic peaks at 320, 335, 350 °C and exothermic peak at 495 °C, respectively, are attributed to the thermal decomposition (endo) and oxidation of organic matter and/or of the gaseous products evolved during the thermal decomposition (exo); with the formation of a mixture of potassium carbonate and carbonaceous residue.

The third mass loss between 650 and 850 °C, with loss of 2.85% corresponding to exothermic peak at 785 and 840 °C are attributed to the oxidation of the carbonaceous residue, remaining potassium carbonate as residue (Calcd. = 65.62%; TG = 66.00%). The endothermic peak at 890 °C is attributed to the melting of the potassium carbonate. The last mass loss above 850 °C, that is also still being observed up to 1000 °C is attributed to the evaporation and/or thermal decomposition of the potassium carbonate.

3.3. Rubidium compound

The TG-DSC curves are shown in Fig. 2(c). The first two mass losses between 40 and 80 and 80–190 °C, corresponding to endothermic peaks at 75 °C and 115, 135 °C respectively are attributed to dehydration with losses of 0.5 and 1.5 H_2O (Calcd. = 3.30 and 9.92%; TG = 3.15 and 9.85%).

The anhydrous compound is stable up to 220 °C and above this temperature the first three mass losses between 220 and 350 °C, 350–430 °C and 430–580 °C, with losses of 31.83%, 5.70% and 2.85% corresponding to exothermic peaks at 310, 330, 420 and 500 °C, respectively are attributed to the oxidation of organic matter and/or of the gaseous products evolved during the thermal decomposition, with the formation of a mixture of rubidium carbonate and carbonaceous residue.

The fourth mass loss between 580 and 720 °C, with loss of 3.62% corresponding to a broad exothermic peak is attributed to the oxidation of the carbonate as residue (Calcd. = 57.65%, TG = 57.00%). The last mass loss above 720 °C, that is still being observed up to 1000 °C is attributed to the evaporation and/or thermal decomposition of the rubidium carbonate. The endothermic peak at 870 °C is attributed to the melting of the rubidium carbonate.

Analysis of the sample holder by energy dispersive X-ray microanalysis (EDX) and field emission scanning electron microscope (SEM) were performed and was noted that, even above 1000 °C, still with mass loss, there corrosion material, as can be seen in Fig. 3; but without evidence of rubidium on the platinum crucible.

3.4. Caesium compound

The TG-DSC curves are shown in Fig. 2(d). The first mass loss that occurs slowly, between 40 and 190 °C corresponding to endothermic peaks at 65, 85 and 180 °C is attributed to dehydration with loss of 1 H_2O (Calcd. = 5.97%, TG = 6.00%).

The second and third mass losses between 190 and 360 °C and 360–500 °C with losses of 26.52% and 10.74%, respectively, corresponding to exothermic peaks at 310, 330, 345 °C and 385, 490 °C are attributed to oxidation of the organic matter and/or of the gaseous products evolved during the thermal decomposition, with the formation of a mixture of caesium carbonate and carbonaceous residue.

The next mass loss between 610 and 730 °C, with loss of 3.48% corresponding to a broad exothermic peak is attributed to the oxidation of, carbonaceous residue, remaining caesium carbonate (Calcd. = 46.07%, TG = 46.74%). The last mass loss between 730 and 950 °C, with loss of 42.14% corresponding a broad endothermic event between 750 and 940 °C is attributed to evaporation and/or thermal decomposition of caesium carbonate, with total loss of 88.88%.

The sample holder was analysed by energy dispersive X-ray microanalysis (EDX) and field emission scanning electron microscope (SEM). Corrosion was observed, without presence of caesium in the platinum crucible, as can be seen in Fig. 4, respectively. These data suggest that in this step occurs the formation of an intermetallic (Pt–Cs) [10], which decompose favouring the formation of PtO_2, as residue [11].

Thus, the endothermic peaks at 790 and 945 °C, are attributed to the melting of caesium carbonate and decomposition of the intermetallic (Pt–CS), respectively.

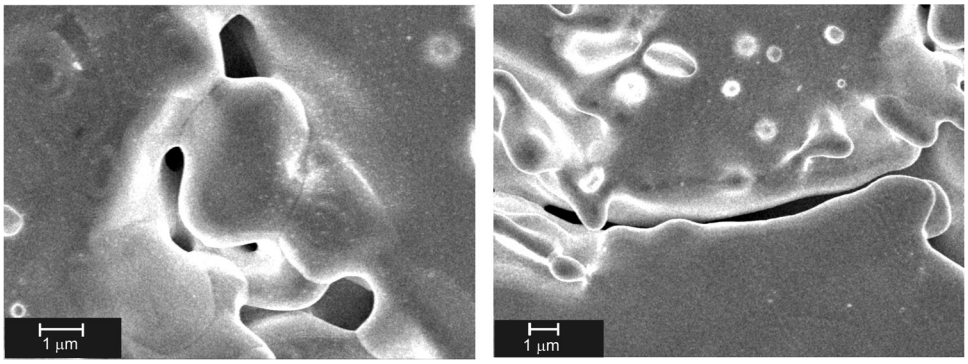

Fig. 3. Analysis of the sample holder by field emission scanning electron microscope (AFM) Rubidium.

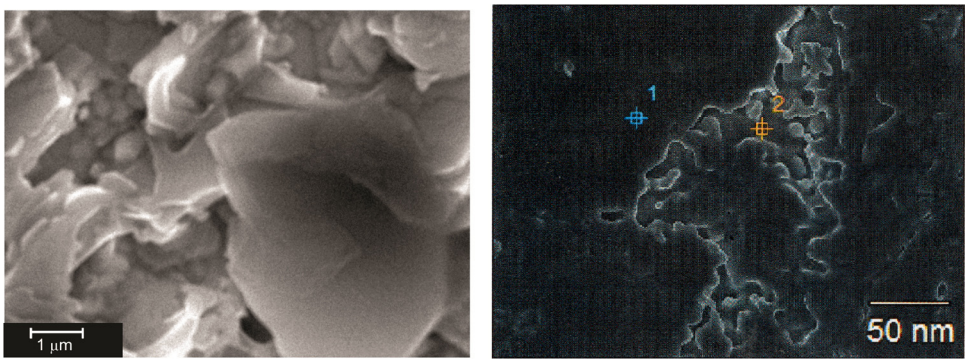

Fig. 4. Energy dispersive X-ray microanalysis (EDX) Caesium.

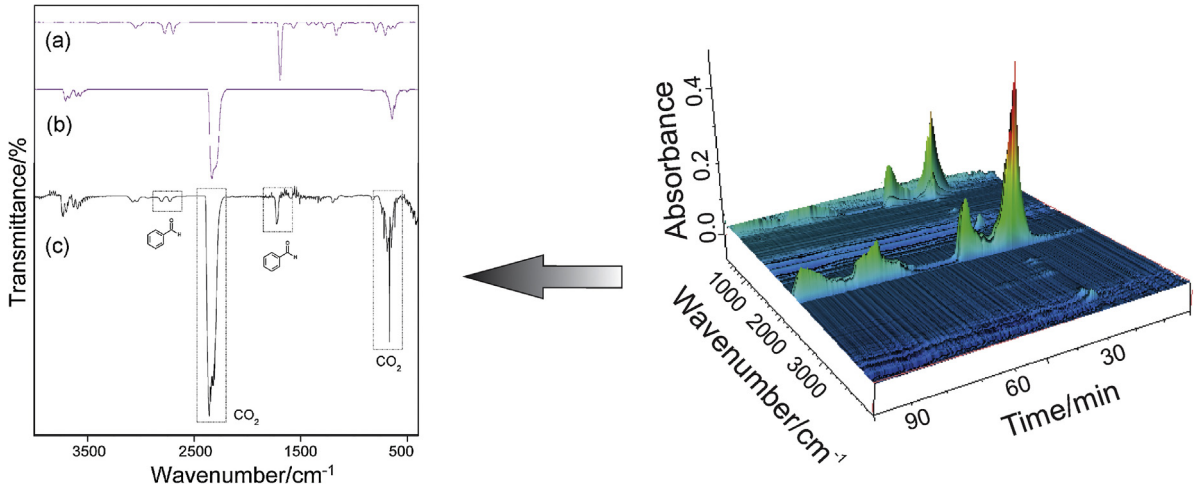

Fig. 5. IR 3D spectra of the gaseous products evolved during the thermal decomposition of potassium mandelate at 390 °C (c). FTIR gases standard of benzaldehyde (a) and CO_2 (b).

In the thermal decomposition of the compounds synthesized in this work, the gaseous products evolved were monitored by FTIR, and they have benzaldehyde and CO_2. The IR spectra of the gaseous products evolved during the thermal decomposition of potassium mandelate, as representative of all compounds, are shown in Fig. 5.

The TG-DSC curves in dynamic dry nitrogen atmosphere are shown in Fig. 6. These curves show mass losses in five or six steps, as observed in dynamic dry air atmosphere and endothermic events corresponding to these losses or due to fusion.

These curves also show that the thermal stability of the anhydrous compounds is higher in nitrogen than in air atmosphere, except for potassium compound which the same thermal stability is observed and they follow the order:

$$Na > K \cong Rb > Cs$$

The TG-DSC curves, as in dynamic dry air atmosphere, show that only caesium compound the final mass loss occurs before 950 °C, while the other compounds, the mass loss is still being observed up to 1000 °C.

For the same compound, the difference in the hydration degree observed in the TG curves in both atmospheres undoubtedly is because these compounds are hygroscopic.

Table 2
Temperature ranges (θ), mass losses (Δm) and peak[a] temperatures (T_p) observed for each step of TG-DSC curves of the compounds in N_2 atmosphere.

Compounds		First	Second	Third	Fourth	Fifth	Sixth
	θ/°C	40–110	260–380	380–460	460–540	540–840	840 to >1000
NaL·0.2 H_2O	Δm/%	1.86	42.08	19.49	4.90	1.60	6.41
	T_p/°C	–	180; 330	–	–	680	930
	θ/°C	75–110	110–165	250–400	400–510	600–895	895 to >1000
KL·0.4H_2O	Δm/%	2.46	1.37	49.00	4.65	7.72	8.5
	T_p/°C	100	–	290, 320	–	700	–
	θ/°C	40–90	90–190	250–370	370–490	490–870	870 to >1000
RbL·0.8H_2O	Δm/%	3.70	9.30	28.58	16.73	12.19	24.40
	T_p/°C	70	115, 130	345	430	670	–
	θ/°C	50–140	200–280	280–470	470–640	640 to >1000	
CsL·0.5H_2O	Δm/%	3.10	6.21	33.86	1.86	38.20	
	T_p/°C	55.80	260	325, 360	590	880, 925	

L = mandelate.
[a] All endothermic peaks.

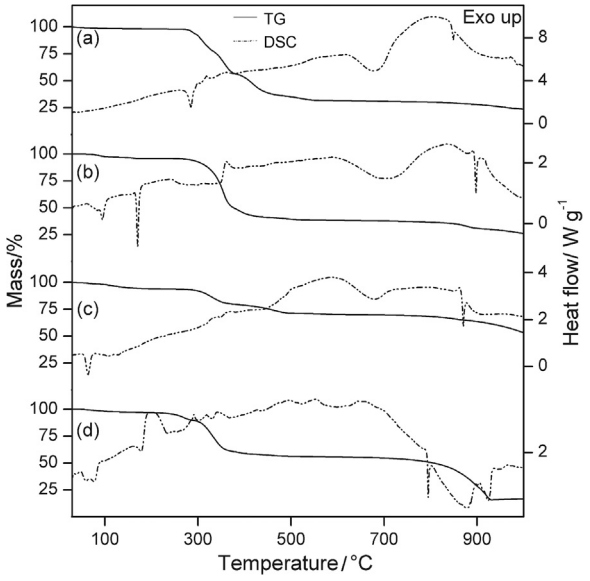

Fig. 6. Simultaneous TG-DSC curves of the compounds: (a) NaL (m = 12.8720 mg), (b) KL (m = 12.1690 mg), (c) RbL (m = 12.5590 mg), (d) CsL (m = 12.0710 mg) under nitrogen atmosphere.

Calculation based on the mass losses up to 840 °C (Na), 895 °C (K), 870 °C (Rb) and 640 °C (Cs) are in agreement with the formation of the respective carbonate, which was confirmed by qualitative test with hydrochloric acid solution on sample heated up to the temperature indicated by the corresponding TG-DSC curves. The endothermic peaks at 280 and 850 °C (Na), 172 and 900 °C (K), 70 and 870 °C (Rb), 180 and 790 °C (Cs) are attributed to fusion of the compound and carbonate, respectively. The temperature ranges (θ), mass losses (m) and peak temperatures observed for each step of the TG-DSC results under N_2 atmosphere, are shown in Table 2.

4. Conclusion

From atomic absorption (AA), thermogravimetric (TG) results, as well as carbon and hydrogen contents determined from TG curve, a general formula could be established for the synthesized compounds.

Rubidium and caesium compounds have high hygroscopicity, thus, the X-ray powder patterns was not obtained, while sodium and potassium ones have a crystalline structure.

The thermal stability of the anhydrous compounds in nitrogen atmosphere is higher than in air one, except for potassium compound.

In both atmosphere (air, N_2), the thermal decomposition of these compounds occurs with the formation of the respective carbonates and except for caesium one the mass loss is still being observed up to 1000 °C.

From EDX and SEM results permitted to verify that the thermal decomposition of rubidium and caesium compounds occurs with the corrosion of the platinum crucible and formation of an intermetallic (Pt–Rb, Pt–Cs), which decompose and/or volatilize, favoring the formation of PtO_2, as residue.

Acknowledgements

The authors thank FAPESP (Proc. 2013/09022-7), CNPq and CAPES Foundations (Brazil) for financial support. Professor Mario Cilence for the EDX and SEM analysis and Professor José Anchieta Gomes Neto for the atomic absorption analysis.

Appendix A. Supplementary data

Supplementary data associated with this article can be found, in the online version, at http://dx.doi.org/10.1016/j.jaap.2015.11.017.

References

[1] P.L. Putten, Mandelic acid and urinary tract infections, Antonie van Leeuwenhoek 45 (1979) 622–623.
[2] A. Fischinger, A. Sarapu, A. Companion, Structural studies on the glycolato, lactato, and mandelato solid complexes of some bivalent iron series metals, Can. J. Chem. 47 (1969) 2629–2637.
[3] P.V. Khadikar, S.D. Chauhan, M.G. Kekre, R.L. America, Infrared spectrum of nickel (II) mandelate complex, Sci. Cult. 37 (1971) 491–492.
[4] D.K. Koppikar, S. Saundararajan, Bonding trends in lanthanide mandelates, Bull. Soc. Chim. Belg. 90 (1981) 1109–1114.
[5] M. Schmidt, A. Schier, H. Schmidbaur, Magnesium bis[D(−)-mandelate] dehydrate and other alkaline earth, alkali and zinc salts of mandelic acid, Z. Naturforsch. 53 (1998) 1098–1102.
[6] R. Carballo, B. Covelo, S. Balboa, A. Castiñeiras, J. Niclos, Mixed-ligand complexes of copper (II) with α-hydroxycarboxylic acids and 1,10-phenanthroline, Z. Anorg. Allg. Chem. 627 (2001) 948–954.
[7] A. Beghidja, S. Hallynck, R. Welter, P. Rabu, Syntheses, structures and magnetic properties of layered metal (II) mandelates, Eur. J. Inorg. Chem. 662 (2005) 662–669.
[8] S. Balboa, R. Carballo, A. Castiñeiras, J.M. Gonzales-Perez, J. Niclós-Gutiérrez, Mononuclear dinuclear and hydroxo-bridged tetranuclear complexesfromreactions of CuII ions mandelic acid and diimineligands, Polyhedron 27 (2008) 2921–2930.
[9] R.C. Silva, F.J. Caires, D.J.C. Gomes, T.A.D. Colman, M. Ionashiro, Synthesis characterization and termal study of solid-state alkaline earth metal mandelates expect beryllium and radium, J. Therm. Anal. Calorim. 117 (2014) 217–221.
[10] O. Loebich Jr., C.J. Raub, Reactions between some alkali and platinum group metals, Platinum Metals Rev. 25 (1981) 113–120.
[11] J.C. Chaston, Reaction of oxygen with platinum metals, Platinum Metals Rev. 8 (1964) 50–54.